Journal of The Electrochemical Society, **154** (4) A337-A342 (2007)
0013-4651/2007/154(4)/A337/6/$20.00 © The Electrochemical Society

Phase Transitions and High-Voltage Electrochemical Behavior of $LiCoO_2$ Thin Films Grown by Pulsed Laser Deposition

H. Xia,[a] L. Lu,[b,z] Y. S. Meng,[c] and G. Ceder[c,*]

[a]*Advanced Materials for Micro- and Nano-System, Singapore-MIT Alliance, Singapore 117576*
[b]*Department of Mechanical Engineering, National University of Singapore, Singapore 117576*
[c]*Department of Materials Science and Engineering, Massachusetts Institute of Technology, Cambridge, Massachusetts 02139, USA*

The phase transitions and electrochemical behavior of $LiCoO_2$ thin-film cathodes prepared by pulsed laser deposition are studied for charging voltages ranging from 4.2 to 4.9 V. Two voltage plateaus at about 4.55 and 4.62 V are observed in the charge-discharge curves. Ex situ X-ray diffraction measurements confirm structural changes and a phase transition from the O3 to the H1-3 phase when $LiCoO_2$ is charged above 4.5 V. Thin-film $LiCoO_2$ electrodes show stable capacity retention up to 4.5 V but significant capacity fade above 4.5 V, which we attribute to damage from strain due to phase transitions and Li gradients. Li diffusion in the Li_xCoO_2 thin film up to 4.5 V is investigated by the potentiostatic intermittent titration technique. The chemical diffusion coefficient of Li reaches the maximum near $x = 0.4$ and starts to decrease when the Li content is further decreased.
 [DOI: 10.1149/1.2509021]

Manuscript submitted September 27, 2006; revised manuscript received November 13, 2006.
Available electronically February 20, 2007.

$LiCoO_2$ is the most commonly used cathode material for rechargeable Li-ion batteries. Though its theoretical capacity is 272 mAh/g, the reversible capacity is limited to 140 mAh/g when the $LiCoO_2$ cathode is cycled between 3 and 4.2 V (measured vs Li metal), corresponding to extracting and inserting about 0.5 Li per $LiCoO_2$. In order to obtain higher capacity from $LiCoO_2$, a cutoff voltage above 4.2 V must be applied, which sometimes results in a rapid capacity loss. Because of the increasing interest in charging $LiCoO_2$ to voltage above 4.2 V, we investigate the kinetics and thermodynamic aspects of Li insertion above 4.2 V. Thin-film electrodes deposited by pulsed laser deposition (PLD) are used in this study as they can be charged and discharged without the need for binder and carbon in the electrode.

Several investigations have identified phase transitions in layered Li_xCoO_2 above 4.5 V.[1-5] Most recently, these transitions were identified as being from the O3 phase to the H1-3 phase around 4.55 V (a stage-two compound) and from the H1-3 phase to the O1 phase (CoO_2) around 4.62 V.[3,5] Some researchers have attributed poor cycling life above 4.2 V to these phase transitions, and argued that they can be inhibited by coating a metal oxide on the surface of $LiCoO_2$.[6-9] Similar improvements in high-voltage cycling after coating $LiCoO_2$ with metal oxides were reported by other groups.[10-13] However, Chen and Dahn et al.[14-16] recently pointed out that mechanical degradation through phase transitions is not a very convincing explanation for loss of capacity because $LiCoO_2$ particles do not expand further and experience no new phase transitions when cycled between 4.2 and 4.4 V. They proposed that the poor capacity retention of $LiCoO_2$ cycled to 4.4 or 4.5 V is caused by impedance growth in the cell, which apparently results from side reactions involving $LiPF_6$-based electrolytes and surface species caused by air or moisture exposure. It has been proven that, with fresh surfaces, $LiCoO_2$ cathodes can be cycled to 4.5 V and deliver a capacity of about 180 mAh/g in a $LiPF_6$-based electrolyte with excellent capacity retention.[17]

Though several groups[1-5] have done excellent work on investigating the electrochemical behavior and structural changes of Li_xCoO_2 above 4.2 V, the Li diffusion in Li_xCoO_2 ($x < 0.5$) above 4.2 V is rarely studied, though a first-principle study[18] has predicted the lithium diffusion in Li_xCoO_2 over the complete composition range $0 < x < 1$.

In this work, we report on the electrochemical behavior of $LiCoO_2$ thin-film cathodes prepared by PLD above 4.2 V. Phase transitions are studied with charge-discharge curves and ex situ X-ray diffraction (XRD). The chemical diffusion coefficient of Li in Li_xCoO_2 is measured up to 4.5 V by potentiostatic intermittent titration technique (PITT).

Experimental

$LiCoO_2$ thin films were grown by PLD on stainless steel (SS) and SiO_2/Si (SOS) substrates at a substrate temperature of 600°C in an oxygen atmosphere of 100 mTorr for 40 min. The PLD target contained 15% excess Li_2O to compensate for lithium loss during the deposition. The target-substrate distance was kept at 40 mm. A Lambda Physik KrF excimer laser beam (248 nm, 150–160 mJ/pulse) was used in the deposition with a repetition frequency of 10 Hz. A double layer of Pt/Ti was deposited on the SOS substrate, where Pt was used as current collector and Ti was used as a buffer layer to enhance the adhesion between the Pt and SiO_2. The thickness of the thin film was estimated from field emission scanning electron microscopy (FESEM, Hitachi S-4100) images for the cross sections of the films on the substrates.

The Li/$LiCoO_2$ cell was assembled with the $LiCoO_2$ thin film as the cathode and a lithium metal foil as the anode and a 1 M $LiPF_6$ in ethyl carbonate-dimethyl carbonate solution (EC/DEC, 1/1 vol %, Ozark Fluorine Specialties, Inc.) as the electrolyte. All electrochemical experiments were conducted in an Ar-filled glove box with a Solatron 1287 two-terminal cell test system. Galvanostatic charge-discharge tests were carried out in different voltage windows with a constant current density of 15 $\mu A/cm^2$. Ex situ XRD measurements of the thin-film cathodes at different charge states were measured using a Shimadzu XRD-6000 X-ray diffractometer with Cu Kα radiation. Data were collected in the 2θ range of 10–70° at a scan rate of 2°/min. To measure the chemical diffusion coefficient of Li in the Li_xCoO_2 film by PITT, a potential step of 10 mV was applied and the current was measured as a function of time. The potential step was stepped to the next level when the current dropped below 0.1 $\mu A/cm^2$. This procedure was repeated between 3.88 and 4.50 V at both increasing and decreasing potentials.

Results

Phase transitions.— In a previous paper,[19] we showed that the very smooth surface of the SOS substrate leads to almost pure (003) texture and better crystallization of the $LiCoO_2$ film resulting in well-defined plateaus in the charge-discharge voltage profiles. Figure 1 shows the charge-discharge curves of the Li/$LiCoO_2$ cell on the SOS substrate in various voltage windows. The lower cutoff voltage was fixed at 3 V and the upper cutoff voltage was varied from 4.2 to 4.9 V. The charge-discharge measurements were con-

* Electrochemical Society Active Member.
z E-mail: mpeluli@nus.edu.sg

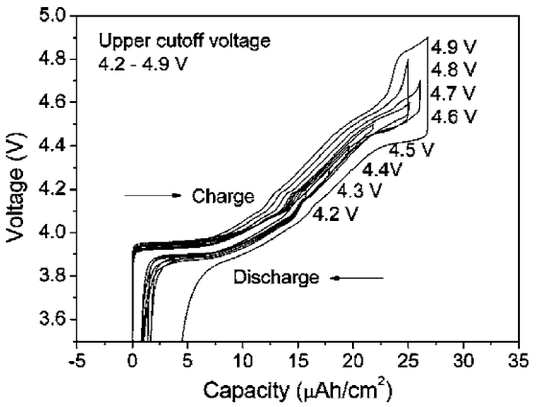

Figure 1. Charge-discharge curves of the Li/$LiCoO_2$ cell with thin-film $LiCoO_2$ cathode using various upper cutoff voltages from 4.2 to 4.8 V. The lower cutoff voltage was fixed at 3 V and the cycling current was 15 μA cm^{-2}.

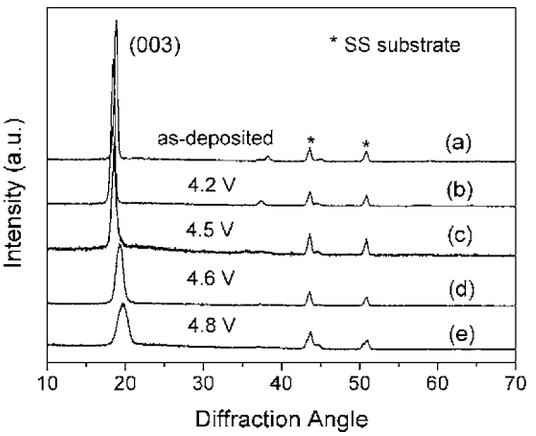

Figure 3. Ex situ XRD spectra for the $LiCoO_2$ films at different charge states: (a) as-deposited, (b) 4.2 V, (c) 4.5 V, (d) 4.6 V, and (e) 4.8 V.

tinuously done on the same cell from 4.2 to 4.9 V. Only one cycle was conducted and recorded for each potential. The thickness of the film was estimated to be about 300 nm from the FESEM on the sample after electrochemical tests. The charge and discharge capacities of the cell increased as the upper cutoff voltage increased up to 4.7 V, similar to what has been found previously on composite electrodes.[5] The polarization of the cell did not change much until 4.5 V. By increasing the upper cutoff voltage from 4.2 to 4.5 V, the capacity increased by 40%, which is slightly higher than what was obtained with the composite electrode (30%).[17] All charge-discharge curves in Fig. 1 show a large plateau at about 3.9 V and two minor plateaus between 4.05 and 4.20 V. The 3.9 V plateau corresponds to the first-order metal-insulator transition,[20,21] and the two minor plateaus correspond to the order-disorder transitions near composition $Li_{0.5}CoO_2$.[22,23] When the upper cutoff voltage was increased to 4.7 V, another two plateaus between 4.5 and 4.7 V could be observed.

The differential capacity curves were derived from the charge-discharge curves from Fig. 1. The peaks in the differential capacity, *dQ*/*dV* (Fig. 2) represent the plateaus in the charge-discharge curves in Fig. 1. No peaks are observed in the voltage range between 4.2 and 4.5 V, indicating that no phase transition occurs in this voltage range. However, the small rise of the *dQ*/*dV* curve at about 4.5 V in the charge process may signify the onset of a phase transition at 4.5 V. When the Li/$LiCoO_2$ cell was charged to 4.7 V, two peaks at 4.55 and 4.62 V were observed, corresponding to the two high-voltage plateaus above 4.5 V in the charge curves in Fig. 1. This observation agrees well with Chen and Dahn's observation on a $LiCoO_2$ composite electrode,[5] who attributed these two peaks to the phase transitions from the O3 phase to the H1-3 phase and from the H1-3 phase to the O1 phase, as predicted by Van der Ven.[3] The O3 and O1 phases are, respectively, the rhombohedral and hexagonal form of Li_xCoO_2, and the H1-3 phase is the stage II compound of Li_xCoO_2, which can be considered as a hybrid of the rhombohedral and hexagonal host. The two peaks in the discharge part of *dQ*/*dV* indicate that the phase transitions at 4.55 and 4.62 V are reversible upon charging to 4.7 V. However, after the Li/$LiCoO_2$ cell was charged to 4.9 V, the two peaks in the discharge part of *dQ*/*dV* merged into one narrow and strong peak, indicating that these reactions are only reversible under certain conditions. The staging of Li in the H1-3 structure was only stable when O3 and O1 stackings alternated along the *c*-axis in the structures. Thus, it is possible that structural damage induced by charging to 4.9 V prevents the Li staging upon discharge. We also found a small peak at about 4.85 V in the charge part of *dQ*/*dV*, similar to the small peak above 5 V found by Chen and Dahn,[5] which they believe is due to the electrolyte decomposition at high voltage. No such peak was found when a solid electrolyte was used,[24] consistent with the assignment of the high-voltage peak to liquid electrolyte decomposition.

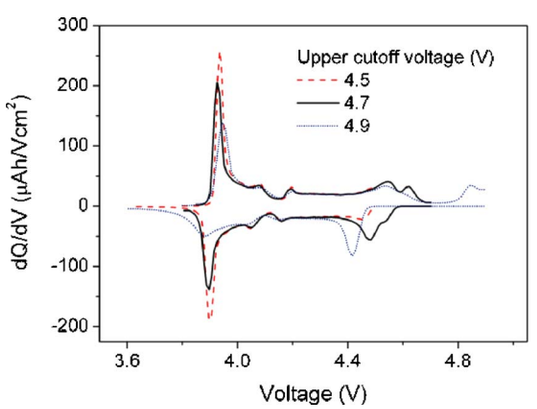

Figure 2. The differential capacity vs voltage for the Li/$LiCoO_2$ cell with different upper cutoff voltages.

To further investigate the two phase transitions between 4.5 and 4.8 V, ex situ XRD experiments were performed on the thin-film $LiCoO_2$ electrodes on SS substrates at different charge states. We prefer films on the SS substrates as they have less diffraction peaks and are easy to assemble and disassemble in our lab-made Swagelok cells. Figure 3 shows selected XRD spectra of the $LiCoO_2$ thin-film electrodes at different charge states from as-deposited ($LiCoO_2$) to 4.8 V. Due to the preferred (003) texture of the film on the SS substrate, the XRD spectrum of the as-deposited $LiCoO_2$ film shows a strong (003) peak. Other reflections have weak intensities. The shift of the (003) peak with different charge states in a selected range of angles is shown in Fig. 4. As shown in Fig. 3, the (003) peak first decreases to a lower angle when charged to 4.2 V, then increases when further charged above 4.2 V and increases significantly when charged above 4.5 V. The ex situ XRD results of $LiCoO_2$ thin film at different charge states agree well with previous reports of ex situ[1] and in situ[2,4,5] XRD of $LiCoO_2$ composite electrodes. As Li is initially removed from $LiCoO_2$, the repulsive interactions between the negatively charged oxygen planes are less compensated by the Li^+–O^{2-} interaction, resulting in an increased *c*-lattice parameter. When the Li content is reduced below $x = 0.5$ (above 4.2 V), the average charge on the oxygen ions decreases and the electrostatic repulsion between the oxygen ions is lowered resulting in a contraction of the host along the *c* axis.[23] Based on the

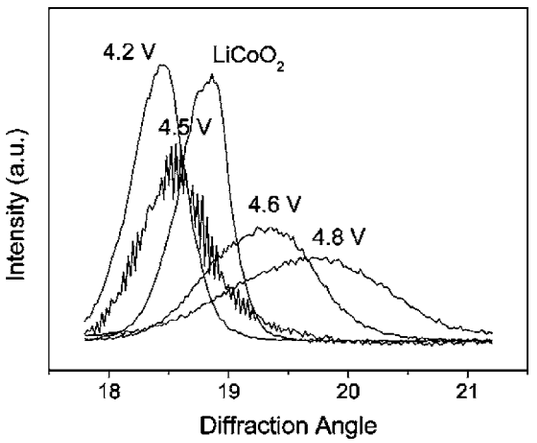

Figure 4. A selected range of the ex situ XRD spectra of the $LiCoO_2$ films at different charge states.

(003) peak position in Fig. 4, the *c*-lattice parameters at different charge states are calculated to be 14.09, 14.42, and 14.31 Å for as-deposited, 4.2, and 4.5 V, respectively. It is obvious that there is a substantial expansion in the *c*-lattice parameter when the film is charged to 4.2 V from the as-deposited state. When the film is further charged to 4.5 V, the *c*-lattice parameter starts to contract. These changes in the *c*-lattice parameter at different charge states are consistent with previous reports.[2,25]

Figure 5 shows ex situ XRD spectra of $LiCoO_2$ films charged to 4.5 and 4.8 V, respectively. In order to detect more diffraction peaks of the $LiCoO_2$ film, we purposely selected the SS substrate with rough surface, which resulted in a more randomly oriented film. All diffraction peaks for the 4.5 V charged material can be indexed based on the O3 structure, in agreement with the electrochemical data, which indicate that at 4.5 V the material still exists in the O3 structure. At 4.8 V our charge-discharge result as well as previous studies[5] indicate that the Li_xCoO_2 film should be fully delithiated and exist in the O1 structure. However, by comparison to the experimental and calculated peak positions for the H1-3 phase in Ref. 5, most diffraction peaks in our film charged to 4.8 V can be indexed as an H1-3 phase but not an O1 phase. The O1 form of CoO_2 only forms when the delithiation of lithium throughout the crystal is completed. Therefore, it may not be possible to detect this final phase through ex situ XRD because any self-discharge will turn the O1 phase into the H1-3 phase. In addition, CoO_2 phase has been

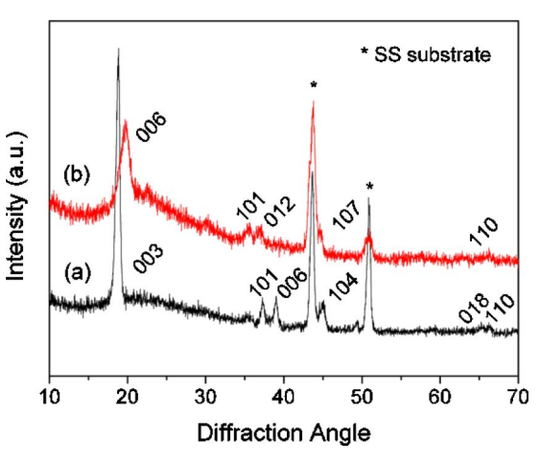

Figure 5. Ex situ XRD spectra for the $LiCoO_2$ films at different charge states: (a) 4.5 V and (b) 4.8 V.

reported to transform to other phases when exposed to air,[2] which also increases the difficulty to detect it by ex situ XRD. Ohzuku et al.,[1] who performed ex situ XRD studies on composite $LiCoO_2$ electrodes, also did not detect the CoO_2 phase.

Capacity retention.— Capacity fade has been extensively investigated in $LiCoO_2$.[7,17,26-29] Possible capacity fade mechanisms have been suggested by different groups. According to Wang et al.,[7] the capacity fade is rapid when cycled to above 4.2 V, and is generally attributed to mechanical failure process associated with structural changes at $x < 0.5$. According to Amatucci[26] and Kim et al.,[27] the fast capacity fade of $LiCoO_2$ electrodes when cycled to 4.4 or 4.5 V is probably due to cobalt dissolution correlated with structural changes. Aurbach et al.,[28] and Chen and Dahn[17] attributed the capacity loss of $LiCoO_2$ electrodes to the impedance growth caused by the formation of a surface layer. Such an electronically resistive surface film may form even quicker when the electrode is cycled to 4.5 V. It seems now generally accepted that below 4.4 or 4.5 V capacity fade is due to impedance growth from side reactions involving $LiPF_6$-based electrolytes and surface species caused by air or moisture exposure. Chen and Dahn[17] indicated that, by creating fresh surfaces, either through grinding or by heating, very good cycle life could be obtained, and they attributed the beneficial effects of coating to the accompanying removal of surface species. Above 4.5 V, the more likely reason for the capacity fade of $LiCoO_2$ is structural phase transitions. According to a transmission electron microscope (TEM) study by Yazami et al.,[29] $LiCoO_2$ electrodes cycled to 4.7 V show an irreversible structural phase transition from hexagonal to cubic spinel, accompanying by increased density of dislocations and internal strains.

Because our $LiCoO_2$ films were grown in a vacuum chamber with in situ heating, without any binder or carbon black, they likely had a fresh surface and are an excellent tool to study the hypothesis of capacity fade. Figure 6a shows the discharge capacity vs cycle number for the Li/$LiCoO_2$ cell ($LiCoO_2$ film on SS substrate) in various voltage windows (10 cycles for each voltage window). Figure 6b shows the capacity fade for the cell as a function of the upper cutoff voltage. It can be seen that the capacity retention of the cell is good for a cutoff voltage below 4.4 V, degrades slightly when cycled to 4.5 V, and significantly deteriorates for voltages above 4.5 V. Ten charge-discharge curves of the cell between 3–4.5 and 3–4.7 V are shown in Fig. 7. The charge-discharge curves of the cell cycled between 3 and 4.7 V show a larger polarization growth with cycling. Figure 8 shows the cycle performance of the cell cycled between 3 and 4.5 V with a constant current of 15 $\mu A/cm^2$ for 50 cycles. The cell exhibits good cycle performance with a capacity fade rate of about 0.2% per cycle. Except for the first several cycles, the charge capacity and discharge capacity are highly reversible with a coulombic efficiency >95%. Jang et al.[24] reported even better cycle performance of their $LiCoO_2$ thin films cycled to 4.4 V in all-solid-state thin-film batteries using the Lipon electrolyte. The improvement of capacity retention is probably because they used solid electrolyte, which avoids the formation of surface films caused by reactions with the liquid electrolyte. In addition, they used a lower cutoff voltage of 4.4 V. Our results seem to give further evidence to the capacity-fade mechanisms previously proposed. Because the thin-film cell has a clean surface, little or no fade exists up to 4.4 to 4.5 V. The structural phase transitions in that regime are mild and accompanied by small changes in lattice parameters. Above 4.5 V, capacity fade is caused by the phase transitions to H1-3 and O1 and occurs in all $LiCoO_2$ electrodes regardless of surface chemistry.

Li diffusion.— Lithium diffusion in the electrode materials is a key factor that determines the rate at which a battery can be charged and discharged. Li diffusion in $LiCoO_2$ has been studied by cyclic voltammetry (CV), electrical impedance spectroscopy (EIS), and potentiostatic intermittent titration technique (PITT).[30-32] However, previous studies of Li diffusion in Li_xCoO_2 have been limited to

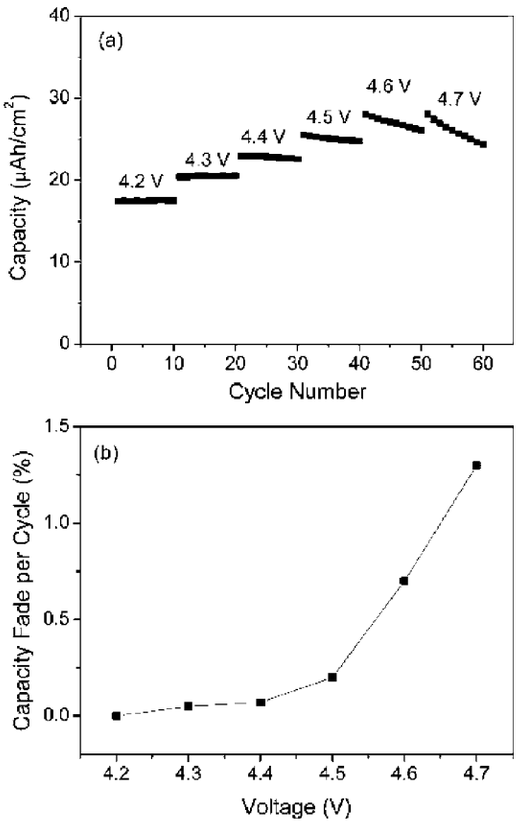

Figure 6. (a) Discharge capacity vs cycle number for the thin-film $LiCoO_2$ electrode with various upper cutoff voltages from 4.2 to 4.7 V and (b) capacity fade per cycle for the thin film $LiCoO_2$ electrode as a function of the upper cutoff voltage.

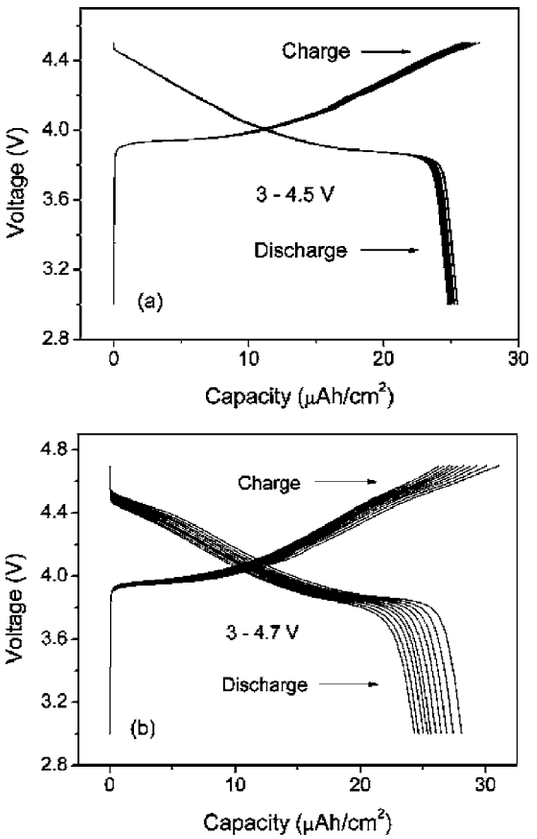

Figure 7. Charge-discharge curves for the thin-film $LiCoO_2$ electrode cycled in different voltage windows: (a) 3–4.5 V and (b) 3–4.7 V.

$x > 0.5$, corresponding to a charge cutoff of about 4.2 V. In this paper we included the region up to $V = 4.5$ V because this potential region could be reversibly accessed in our thin-film electrodes. The chemical diffusion coefficients of Li were measured using PITT. In a single phase region, the current after each potential step decayed exponentially with time according to the expression

$$I(t) = \frac{2Fa(C_S - C_0)\tilde{D}}{L} \exp\left(-\frac{\pi^2 \tilde{D} t}{4L^2}\right) \quad [1]$$

Here, F is the Faraday constant, a is the active surface area of the electrode, L is the thickness of the cathode film, and $(C_s\text{-}C_0)$ is the change in Li concentration at the cathode-electrolyte interface during each potential step. The chemical diffusion coefficient, $\tilde{D}_{Li}$, can be calculated from the slope of the linear region in the plot of $\ln[I(t)]$ vs t, where

$$\tilde{D} = -\frac{d\ln(I)}{dt}\frac{4L^2}{\pi^2} \quad [2]$$

Figure 9a shows the chemical diffusion coefficients obtained from PITT as a function of electrode potential during both charge and discharge. The values of $\tilde{D}_{Li}$ in the potential range between 3.88 and 4.50 V vary from 10^{-12} to 10^{-11} cm^2 s^{-1}, similar to values obtained previously in the potential range between 3.88 and 4.20 V.[31,32] Three minima exist in $\tilde{D}_{Li}$ near 3.9, 4.1, and 4.2 V, respectively. The minimum near 3.9 V is due to the two-phase region and the standard Cottrell analysis to extract $\tilde{D}_{Li}$ may not be appropriate.[33] The other two minima near 4.1 and 4.2 V are associated with the order-disorder phase transitions near $Li_{0.5}CoO_2$. Such minima were also observed in Jang's report, and in our previous study.[32,34] Figure 9b shows $\tilde{D}_{Li}$ vs x of Li_xCoO_2 in the composition region $0.14 < x < 0.75$. The chemical diffusion coefficient of Li initially increases with decreasing Li content, is maximal at about $x = 0.4$, and then starts to decrease with decreasing Li content. The chemical diffusion coefficient of Li in Li_xCoO_2 is expected to be influenced by several factors: (*i*) the concentration of vacancy sites available for lithium ions, (*ii*) the activation barrier for lithium ions to jump, and (*iii*) the thermodynamic factor. The concentration of vacancy sites increases with decreasing Li content. As discussed by Van den Ven and

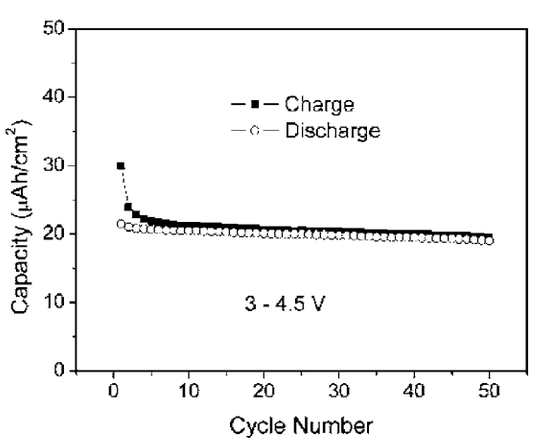

Figure 8. Charge-discharge capacities vs cycle number for the thin-film $LiCoO_2$ electrode cycled between 3 and 4.5 V with a current of 15 μA cm^{-2}.

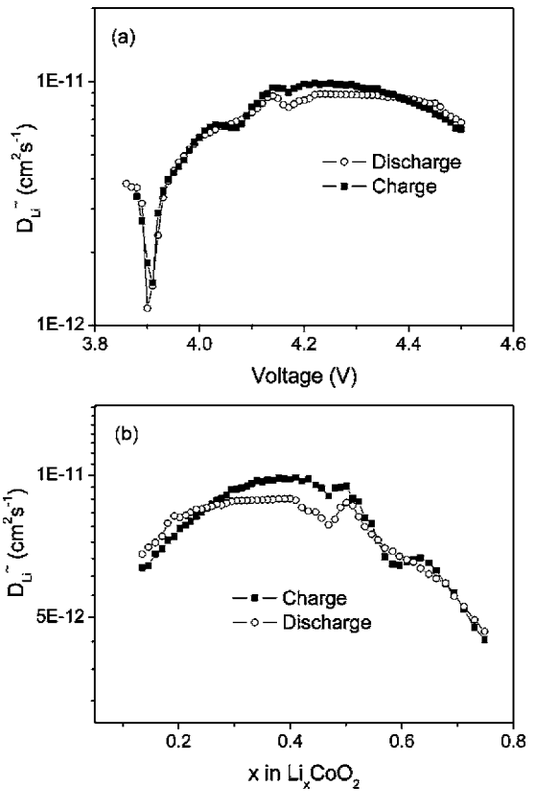

Figure 9. (a) Chemical diffusion coefficients of Li vs potential during charge and discharge states and (b) chemical diffusion coefficients of Li vs x in Li_xCoO_2 during charge and discharge states as obtained with PITT.

Ceder,[18] the variation of the activation barrier can be attributed to two factors. One is the c-lattice parameter. A drop of the c-lattice parameter reduces the distance between the oxygen planes, and compresses the tetrahedral site, resulting in an increase in the activation barrier. A second factor is the change in effective valence of the cobalt ions with x. As x is reduced, the effective positive charge on Co increases, causing the activation barrier to increase.[18,35] The thermodynamic factor is a measure of the deviation of the chemical potential from that for an ideal solution. In the composition range $0.5 < x < 0.75$, the c-lattice parameter increases only slightly with decreasing Li content and the activation barrier does not change much.[18] Therefore, in this composition range, the chemical diffusion coefficient of Li is mainly influenced by the increasing concentration of Li vacancies. For $x < 0.5$, the c-lattice parameter decreases, and the charge on Co increases with decreasing Li content, resulting in a significant increase in the activation barrier energy.[18]

Though there is a good agreement between the experimental result and previously calculated results[18] for the Li diffusivity in $LiCoO_2$, some discrepancies exist. The experimental result shows a maximum at about $x = 0.5$, whereas the calculation result shows a minimum at about $x = 0.5$. The chemical diffusion coefficient $\tilde{D}_{Li}$ is a product of the self-diffusion coefficient D_{Li} and the thermodynamic factor Θ.[36] Θ is proportional to $-dV/dx$, which will have minima at the phase boundaries near the composition $Li_{0.5}CoO_2$ and a maximum at composition $Li_{0.5}CoO_2$. As discussed by Van der Ven and Ceder,[18] the self-diffusion coefficient, D_{Li}, should have a minimum at $x = 0.5$ due to the higher activation energy associated with Li jumps in ordered $Li_{0.5}CoO_2$. Whether the chemical diffusivity, $\tilde{D}_{Li}$, is maximal or minimal depends on the balance between the thermodynamic factor and the self-diffusion coefficient. A less-ordered $Li_{0.5}CoO_2$ cathode will exhibit a less deep minimum of D_{Li}, as there would be less limitation to Li jumping. The thermodynamic factor, is an averaged quantity and is likely to be less drastically influenced by the state of order. Hence, in real samples, which are less ordered than in simulations,[32] the thermodynamic factor may dominate and lead to a maximum. For both experimental and calculation results, $\tilde{D}_{Li}$ starts to drop with decreasing x when $x < 0.4$. However, the drop of $\tilde{D}_{Li}$ in the calculation result is much more pronounced than in the experiments. We attribute this discrepancy to the difference of c-lattice parameter change between calculations and experiments. In previous first- principle calculation,[23] the calculated c-lattice parameter of the O3 host is systematically smaller than the experimentally observed value by approximately 4% and drops more significantly in the composition region $0.15 < x < 0.5$ than in our experimental results: In the calculated result, the c-lattice parameter changes from 13.8 to 12.9 Å when x decreases from 0.5 to 0.15. For our thin-film experimental result, the c-lattice parameter changes from 14.42 to 14.31 Å when x decreases from 0.5 to 0.15 (4.2 to 4.5 V). This large discrepancy is likely due to the overestimation of the van der Waals forces in the local density approximation, which keeps the oxygen layers together as Li is removed.

Discussion

Our thin-film $LiCoO_2$ electrodes show electrochemical behavior that is consistent with composite $LiCoO_2$ electrodes studied previously.[2,5] Two voltage plateaus between 4.5 and 4.7 V are observed for both charge and discharge curves, which likely correspond to the O3 to the H1-3, and the H1-3 to the O1 transitions. We find that the stability of these two phase transitions is highly dependent on the cutoff voltage. As shown in Fig. 2, two peaks between 4.5 and 4.7 V can be observed for both charge and discharge when using the cutoff voltage of 4.7 V. After the cutoff voltage has been raised to 4.9 V, the two peaks for the charge become weak, and the two peaks for the discharge become one narrow and strong peak. The increased difference between these two peaks for charge and discharge indicates that the irreversibility of these two reactions increases as the cutoff voltage increases. We also find that charging the film to very high voltage such as 4.9 V will induce further damage to the structure of the film. As shown in the dQ/dV curve for 4.9 V in Fig. 2, besides the changes of the two peaks at high voltage, the 3.9, 4.1, and 4.2 V peaks all become broad and weak for the discharge process. Especially, the 3.9 V peak for the discharge is much weaker than that for the charge, which indicates that dramatic structure degradation occurs when the film is charged to 4.9 V. As shown in Fig. 1, the polarization of the cell increases gradually as the cutoff voltage is increased from 4.5 to 4.8 V. However, a sudden increase of the cell polarization occurs with a dramatic increase of irreversible capacity when the cutoff voltage is increased from 4.8 to 4.9 V. At the same time, there is a new voltage plateau emerging at about 4.85 V for the charge, which can be attributed to electrolyte decomposition. In this case, we speculate that the electrolyte decomposition probably accelerates the degradation of the crystal structure of the film or impedance growth at the interface between the film and electrolyte and contributes to the large polarization of the cell.

Our work confirms the results obtained by Chen and Dahn,[17] which attributed capacity fade for $LiCoO_2$ electrodes cycled at voltage <4.5 V to the impedance growth of the cell induced by the formation of a surface layer, and not to phase transformations. In agreement, we find that structural changes between 4.2 and 4.5 V are small and that the order-disorder transitions, which occur at 4.1 and 4.2 V, are reversible. The fact that the lattice parameters change little between 4.2 and 4.5 V, and that the Li diffusivity is high, makes it unlikely that capacity degradation through mechanical stress occurs in this voltage region, which is further confirmed by our cycling tests. Below 4.5 V (Fig. 6), very little capacity loss is observed. Because the surfaces of our $LiCoO_2$ films are likely to be

free of contamination, the lack of capacity loss between 4.2 and 4.5 V seems consistent with the mechanism proposed by Aurbach et al.[28] and Dahn and Chen.[17]

Rapid capacity fade is found when $LiCoO_2$ is cycled to higher voltages such as 4.6 or 4.7 V. In this voltage regime phase transitions occur with a substantial effect on the lattice parameters. Phase transitions together with the decreasing Li diffusivity, which makes Li composition gradients larger, likely leads to large internal strains, and subsequent mechanical degradation of the material. The above conclusion is evidenced in our materials by the lack of clear phase transitions in the charge-discharge cycle after exposure to high potential. Li vacancy ordering is likely to be most sensitive to structure defects. It is therefore not surprising that the plateaus at 4.1 and 4.2 V are significantly deteriorated after a charge to 4.9 V. Yazami et al.,[29] as well as Wang et al.,[7] observed significant amounts of cracking, dislocations, and other extended defects in samples charged to high potential. Cumulative damage of this nature may be responsible for capacity fade during overcharging or in long-term cycling of $LiCoO_2$ electrodes. In addition, CoO_2 has been reported to decompose through loss of oxygen, and the decomposition of CoO_2 may also contribute to the capacity fade when $LiCoO_2$ cycled to 4.7 V.

Lattice parameter changes due to phase transitions or compositional variations are most detrimental when they occur with high Li composition gradients, as this leads to large compatibility strains in the crystallites. Li diffusivity is the key factor which controls the homogeneity (at the particle level) of the charge-discharge process. We observe a drop of the Li chemical diffusion coefficient in Li_xCoO_2 for $x < 0.4$, which is probably caused by the drop of *c*-lattice parameter and the increased charge on Co. Though it is difficult to measure the chemical diffusion coefficient of Li above 4.5 V (PITT is only meaningful in a single phase region), it is reasonable to believe that an even faster drop of the Li diffusion will occur when the $LiCoO_2$ film is further charged to 4.6 or 4.7 V. According to both experimental[2] and calculation[3] results, the *c*-lattice drops more significantly when $LiCoO_2$ goes through the two phase transitions from the O3 to the H1-3 phase and from the H1-3 to the O1 phase. As discussed previously, a drop of the *c*-lattice parameter slows down the Li diffusion. Therefore, the sluggish Li diffusion accompanying the large internal strains above 4.5 V for $LiCoO_2$ may limit the use of $LiCoO_2$ electrodes at high voltages above 4.5 V.

Conclusions

We have used thin-film $LiCoO_2$ electrodes without binder or carbon to study the phase transitions, Li diffusion, and capacity fade above 4.2 V. Two voltage plateaus above 4.5 V are observed in the charge-discharge curves. Ex situ XRD indicated that one of these phase transitions converts the O3 into the H1-3 phase. The $LiCoO_2$ film shows good capacity retention up to a cutoff voltage of 4.5 V, but rapid capacity fade occurs when cycled to 4.6 or 4.7 V. The structural changes between 4.2 and 4.5 V have no obvious effect on the capacity fade, while the structural changes between 4.5 and 4.7 V combined with the decrease of Li diffusivity probably lead to the fast capacity fade of $LiCoO_2$ when cycled to such a high voltage. The chemical diffusion coefficient of Li in Li_xCoO_2 decreases with decreasing Li content for $0.14 < x < 0.4$. The decrease of the chemical diffusion coefficient of Li in Li_xCoO_2 is attributed to the increase of activation barrier of Li jumping at low Li content. An even faster drop of Li diffusion is likely to occur at voltage above 4.5 V. Our present studies provide further evidence that it is very possible to raise the cutoff voltage of $LiCoO_2$ to 4.5 V without sacrificing the capacity retention.

Acknowledgments

This research was supported by Advanced Materials for Micro- and Nano- System (AMM&NS) program under Singapore-MIT Alliance (SMA) and by National University of Singapore.

National University of Singapore assisted in meeting the publication costs of this article.

References

1. T. Ohzuku and A. Ueda, *J. Electrochem. Soc.*, **141**, 2972 (1994).
2. G. G. Amatucci, J. M. Tarascon, and L. C. Klein, *J. Electrochem. Soc.*, **143**, 1114 (1996).
3. A. Van der Ven, M. K. Aydinol, and G. Ceder, *J. Electrochem. Soc.*, **145**, 2149 (1998).
4. X. Sun, X. Q. Yang, J. McBreen, Y. Gao, M. V. Yakovleva, X. K. Xing, and M. L. Daroux, *J. Power Sources*, **97–98**, 374 (2001).
5. Z. H. Chen, Z. H. Lu, and J. R. Dahn, *J. Electrochem. Soc.*, **149**, A1604 (2002).
6. T. Ohzuku, A. Ueda, M. Nagayama, Y. Iwakoshi, and H. Komori, *Electrochim. Acta*, **38**, 1159 (1993).
7. H. Wang, Y. Jang, B. Huang, D. R. Sadoway, and Y. Chang, *J. Electrochem. Soc.*, **146**, 473 (1999).
8. J. Cho, Y. J. Kim, T. J. Kim, and B. Park, *Angew. Chem., Int. Ed.*, **40**, 3367 (2001).
9. J. Cho and G. Kim, *Electrochem. Solid-State Lett.*, **2**, 253 (1999).
10. Z. Wang, C. Wu, L. Liu, L. Chen, and X. Huang, *Solid State Ionics*, **148**, 335 (2002).
11. Z. Wang, C. Wu, L. Liu, L. Chen, and X. Huang, *J. Electrochem. Soc.*, **149**, A466 (2002).
12. L. Liu, Z. Wang, F. Wu, L. Chen, and X. Huang, *Solid State Ionics*, **152**, 341 (2002).
13. A. M. Kannan, L. Rabenberg, and A. Manthiram, *Electrochem. Solid-State Lett.*, **7**, A16 (2002).
14. Z. H. Chen and J. R. Dahn, *Electrochem. Solid-State Lett.*, **5**, A213 (2002).
15. Z. H. Chen and J. R. Dahn, *Electrochem. Solid-State Lett.*, **6**, A221 (2003).
16. Z. H. Chen and J. R. Dahn, *Electrochem. Solid-State Lett.*, **7**, A11 (2004).
17. Z. H. Chen and J. R. Dahn, *Electrochim. Acta*, **49**, 1079 (2004).
18. A. Van der Ven and G. Ceder, *Electrochem. Solid-State Lett.*, **3**, 301 (2000).
19. H. Xia, L. Lu, and G. Ceder, *J. Alloys Compd.*, **417**, 304 (2006).
20. C. A. Maianetti, G. Kotliar, and G. Ceder, *Nat. Mater.*, **3**, 627 (2004).
21. J. Molenda, A. Stoklosa, and T. Bak, *Solid State Ionics*, **36**, 53 (1989).
22. J. N. Reimers, J. R. Dahn, and U. von Sacken, *J. Electrochem. Soc.*, **140**, 2091 (1992).
23. A. Van der Ven, M. K. Aydinol, and G. Ceder, *Phys. Rev. B*, **58**, 2975 (1998).
24. Y. I. Jang, N. J. Dudney, D. A. Blom, and L. F. Allard, *J. Power Sources*, **119–121**, 295 (2003).
25. J. Cho, Y. J. Kim, and B. Park, *Chem. Mater.*, **12**, 3788 (2000).
26. G. G. Amatucci, J. M. Tarascon, and L. C. Klein, *Solid State Ionics*, **83**, 167 (1996).
27. Y. J. Kim, H. Kim, B. Kim, D. Ahn, J. G. Lee, T. J. Kim, D. Son, J. Cho, Y. W. Kim, and B. Park, *Chem. Mater.*, **15**, 1505 (2003).
28. D. Aurbach, B. Markovsky, A. Rodkin, E. Levi, Y. S. Cohen, H. J. Kim, and M. Schmidt, *Electrochim. Acta*, **47**, 4291 (2002).
29. R. Yazami, Y. Ozawa, H. Gabrisch, and B. Fultz, *Electrochim. Acta*, **50**, 385 (2004).
30. Y. Iriyama, M. Inaba, T. Abe, and Z. Ogumi, *J. Power Sources*, **94**, 175 (2001).
31. M. D. Levi, G. Salitra, B. Markovsky, H. Teller, D. Aurbach, U. Heider, and L. Heider, *J. Electrochem. Soc.*, **146**, 1279 (1999).
32. Y. I. Jang, B. J. Neudecker, and N. J. Dudney, *Electrochem. Solid-State Lett.*, **4**, A74 (2001).
33. B. C. Han, A. Van der Ven, D. Morgan, and G. Ceder, *Electrochim. Acta*, **49**, 4691 (2004).
34. H. Xia, L. Lu, and G. Ceder, *J. Power Sources*, **159**, 1422 (2006).
35. K. Kang, Y. S. Meng, J. Breger, C. P. Grey, and G. Ceder, *Science*, **311**, 977 (2006).
36. W. Wepppner and R. A. Huggins, *J. Electrochem. Soc.*, **124**, 1569 (1977).